Analysis of Unsteady Airloads of Helicopter Rotors in Hover

Balusu M. Rao*
Analytical Methods, Inc., Bellevue, Wash.
and
Paul R. Schatzle†
Texas A&M University, College Station, Texas

A numerical lifting surface method based on the velocity potential has been developed for predicting the unsteady airloads on a hovering rotor in compressible flow using a realistic representation of the wake, Landgrebe's empirical model. The steady-state loads compare reasonably well with available results for four-bladed rotors, while the spanwise variation of the unsteady aerodynamic derivatives obtained shows a characteristic peak in the outboard region of the blade due to the presence of the tip vortex.

Nomenclature

a	= speed of sound
A	= surface influence coefficient
B	= wake influence coefficient
c	= blade chord
C	= generalized influence coefficient
C_L	= unsteady lift coefficient
$C_{mc/2}$	= unsteady moment coefficient about midchord axis
C_T	= rotor thrust coefficient
e	= flapping hinge offset
$f(y)$	= flapping mode relative to tip
$F(y)$	= torsional mode relative to tip
k,K	= doublet intensity
l	= reference length (semichord)
$\bar{l}$	= local lift (pressure distribution)
L'	= lift per unit span
M	= Mach number
$M'_{c/2}$	= moment per unit span about midchord axis, nose-up positive
N_R	= rotor r.p.m.
NB	= number of blades in rotor
p	= frequency of oscillation
$Q(=\nabla\phi)$	= total velocity at a point
R	= rotor radius
S	= surface area in transformed coordinates; streamwise distance along a wake strip in transformed coordinates
U	= local velocity
U_t	= reference (tip) velocity
$\tilde{w},\tilde{W}$	= downwash velocity
(x,y,z,t)	= Cartesian coordinates and time
(X,Y,Z,T)	= transformed coordinates and time
α	= blade angle of attack
β	$=(1-M^2)^{1/2}$
β_c	= coning angle
$\epsilon(=p/\Omega)$	= frequency ratio
ζ	= vertical displacement of a point on the blade
θ_t	= blade twist – negative when α decreases along the span
θ_r	= collective pitch angle at blade root
κ	$=M\omega/\beta^2$
λ	$=M^2\omega/\beta^2$
ν	$=\omega/\beta^2$
ξ	= distance from a field point to collocation point in transformed coordinates
ρ	= air mass density
σ	= rotor solidity
$\tilde{\phi},\tilde{\Phi}$	= velocity potential
$\omega(=pl/U)$	= reduced frequency
Ω	= rotor angular velocity
∇	= gradient operator in Cartesian coordinates
∇^2	= Laplacian in Cartesian coordinates
$\bar{\nabla}^2$	= Laplacian in transformed coordinates

Superscripts

~	= indicates a perturbation quantity
′	= amplitude of a harmonic function

Subscripts

c	= coning
co	= root cut-out
$c/2$	= semichord axis
f	= flapping motion
mn	= surface panel
n	= wake strip
p	= collocation point
s	= steady-state condition
t	= twisting motion
te	= trailing edge
z	= flapping motion
α	= torsional motion

Presented as Paper 77-159 at the AIAA 15th Aerospace Sciences Meeting, Los Angeles, Calif., Jan. 24-26, 1977; submitted Feb. 4, 1977; revision received Jan. 9, 1978.

Index categories: Helicopters; Propeller and Rotor Systems; Nonsteady Aerodynamics.

*Senior Research Scientist. Member AIAA.

†Graduate Research Assistant, Dept. of Aerospace Engineering.

Introduction

MORE papers have been published on the subject of unsteady aerodynamics of rotor blades during the last two decades than in all the earlier years of helicopter development. In earlier work, attention was focused on vibration problems which often limit helicopter performance. With the advent of high-speed helicopters, it has also become important to study compressibility effects and blade flutter problems. In Ref. 1, a detailed account was given of the significant developments in the field of unsteady aerodynamics of rotor blades. Accurate prediction of the unsteady airloads has required the use of a realistic wake geometry representation, compressibility effects, and chordwise load distribution. Most of the methods to date have employed several simplifying assumptions regarding either the rotor or wake geometry.

It has been known for a long time that the proximity of the helical wake is a contributing factor to blade flutter. For the case of low inflow, the wake is closely coiled under the rotor disk and it could have a strong influence on the aerodynamic forces acting on a blade. For low-inflow conditions, Loewy[2] approximated the complex helical flowfield beneath the rotor disk by an infinite system of rectilinear vortex filaments and calculated the spanwise loading on the blade assuming local two-dimensional, incompressible flow. He was able to obtain a special function, similar to that of Theodorsen's function for a simple airfoil in straight flow, for the aerodynamic forces on a typical blade section as a function of reduced frequency, the frequency ratio p/Ω, and wake spacing. Later, J. P. Jones[3] treated the case of a single-bladed rotor in incompressible flow using a mathematical model similar to that of Loewy's, and determined that the rotor wake was responsible for some of the vibratory loading observed on actual rotors. Timman and Van deVooren[4], on the other hand, assumed that there was no inflow through the rotor disk and developed a theory for calculating the aerodynamic forces on a blade rotating through its own wake. Their results agree with those obtained by Loewy[2] and Jones[3] for zero wake spacing.

All of the theoretical work just described is based on the assumption that the flow is incompressible. Jones and Rao[5] applied the theory of Jones[6] for a single airfoil in compressible flow to Loewy's two-dimensional mathematical model and developed a theory for an oscillating rotor blade in compressible flow. The values of the aerodynamic coefficients agree with those obtained by Loewy[2] and J. P. Jones[3] for zero Mach number but differ appreciably as the Mach number is varied. Hammond[7] also developed a theory for determining compressibility effects, using a model in which the wake of the qth blade of a Q-bladed rotor after n revolutions extends from $-2\pi\ (n+q/Q)$ to ∞; in Jones and Rao's model it extends from $-\infty$ to ∞. His aerodynamic coefficients for several Mach numbers and inflow ratios are in general agreement with the results for Jones and Rao. In a very recent paper,[8] the various existing unsteady aerodynamic strip theories for both fixed- and rotary-wing aeroelastic analyses were modified so as to make them applicable to the coupled flap-lag-torsional aeroelastic problem of a rotor blade in hover. The modified strip theories were incorporated in a coupled flap-lag-torsional aeroelastic analysis of the rotor blade in hover and the sensitivity of the aeroelastic stability boundaries to the aeroelastic analyses were examined.

While the aerodynamic derivatives predicted by two-dimensional strip theories are widely used in predicting the flutter speeds of helicopter rotor blades, the methods do not allow for curvature and finite aspect ratio effects. Jones and Rao[9] studied tip-vortex effects in compressible flow as a correction to the two-dimensional flow and concluded that they are negligible except in regions close to the tip. The earlier attempts to include the tip vortices in a truly three-dimensional fashion involved a helical wake representation below the rotor blade in hover and a skewed helical pattern for forward flight. Miller[10] developed a helical wake model in which the rotor wake was divided into a "near" wake and a "far" wake. The near wake included the portion attached to the blade that extends approximately one-quarter of a revolution from the blade trailing edge. The effects of the near wake include an induced chordwise variation in downwash and were formulated using an adaptation of Loewy's strip theory. The chordwise variation in the velocity over the airfoil induced by the far wake was neglected. He showed that under certain conditions of low inflow and low-speed transition flight, the returning wake could be sucked up into the leading edge of the rotor, which would account for some of the vibration and noise. Piziali[11] has developed an alternative numerical method in which the wake of a rotor blade is represented by discrete straight-line shed and trailing vortex elements. He satisfied the chordwise boundary conditions, but the rotor blade was limited to one degree of freedom in flapping. Sadler,[12] using a model similar to Piziali's, developed a method for predicting the helicopter wake geometry at a "start-up" configuration. He represented the wake by a fine mesh of transverse and trailing vortices starting with the first movement of the rotor blade generating a bound vortex, and, to preserve zero total vorticity, a corresponding shed vortex in the wake. Integrating the mutual interference of the trailing and shed vortices upon each other over small intervals of time, Sadler was able to predict a wake geometry. Although his model showed fair agreement with the available experimental data for advance ratios above 1/10, Sadler's method is limited due to the large computational time required to represent the wake by a fine mesh. Recently, Rao and Jones[13] developed a simple but general numerical lifting surface method for predicting unsteady airloads on a single-bladed rotor blade in compressible flow on a full three-dimensional basis. The numerical method was based on the velocity potential formulation and classical wake representation. The comparisons indicated the inadequacies of strip theory for airload distribution and an important conclusion drawn from this study was that the curved wake has a substantial effect on the chordwise load distribution. Jenney et al.[14] computed rotor hover performance using a lifting line approach for steady incompressible flow, and modeled the wake as a finite number of vortex segments trailing in a roughly helical path beneath the rotor. Their results pointed out the necessity of including the radial contraction of the wake near the rotor. Subsequently, Landgrebe[15] conducted an extensive analytical and experimental investigation to obtain model rotor hover performance and wake geometry data for a wide range of operating conditions. He was able to describe the wake geometry for any hover condition by a set of simple empirical equations and show that the experimental wake geometry could be used to predict hover performance which correlated well with experiment.

In a recent report,[16] a numerical lifting surface method was applied to predict the unsteady airloads on a multibladed helicopter rotor in hover using a realistic wake representation. The method employed a velocity potential formulation and the wake geometry was prescribed using Landgrebe's model. In this paper the numerical lifting surface method developed in Ref. 16 is described and some typical unsteady airload results are presented. It should be stressed that the lifting surface method employed is strictly valid only for fixed wings in rectilinear flight; its present use is therefore approximate.

Basic Equations

The governing equation for the unsteady compressible three-dimensional flow of an isentropic inviscid irrotational fluid is given in terms of its velocity potential by

$$a^2\nabla^2\phi=\frac{\partial^2\phi}{\partial t^2}+\frac{\partial Q^2}{\partial t}+Q\cdot\nabla\left(\frac{Q^2}{2}\right) \tag{1}$$

For uniform rectilinear flow the total potential consists of the freestream and perturbation potentials, i.e.,

$$\phi=Ux+\tilde{\phi} \tag{2}$$

such that Eq. (1) may be written

$$(1-M^2)\tilde{\phi}_{xx}+\tilde{\phi}_{yy}+\tilde{\phi}_{zz}=\frac{1}{a^2}\tilde{\phi}_{tt}+\frac{2M}{a^2}\tilde{\phi}_{xt} \tag{3}$$

Adopting the procedure of Jones,[18] let a coordinate transformation be made such that

$$X=\frac{x}{l} \qquad Y=\beta\frac{y}{l} \qquad Z=\beta\frac{z}{l} \qquad T=\frac{Ut}{l} \tag{4}$$

Furthermore, let the perturbation potential be transformed according to the relation

$$\tilde{\phi}(x,y,z,t)=Ul\tilde{\Phi}(X,Y,Z,T)e^{i(\lambda X+\omega T)} \tag{5}$$

Equations (3-5) may then be combined to yield

$$\bar{\nabla}^2\tilde{\Phi}+\kappa^2\tilde{\Phi}=0 \tag{6}$$

which is simply Helmholtz's equation for the perturbation potential in the transformed coordinate system. As shown in Ref. 16, Eq. (6) may be used in conjunction with Green's theorem to derive a relation between the downwash velocity at a point on a wing and a distribution of doublets over the wing and wake surfaces, i.e.,

$$4\pi\tilde{W}_p=\int\int K\frac{\partial^2}{\partial Z^2}\left(\frac{e^{-i\kappa\xi}}{\xi}\right)\mathrm{d}S \tag{7}$$

where K, the local doublet intensity, is equal to the discontinuity in the transformed potential across the wing or wake. The value of K at a point in the wake may be determined from the value of K at the trailing edge of the wing in the following manner. From Euler's equation, the local pressure difference across a thin surface is related to the corresponding discontinuity in potential by

$$\tilde{l}=\rho\left(\frac{\partial k}{\partial t}+U\frac{\partial k}{\partial x}\right) \tag{8}$$

which becomes

$$\tilde{l}=\rho U^2\left(i\nu K+\frac{\partial K}{\partial X}\right)e^{i(\lambda X+\omega T)} \tag{9}$$

when combined with Eqs. (4) and (5). Since the wake cannot support a pressure discontinuity, $\tilde{l}=0$ in Eq. (9) and, thus,

$$K(X,Y)=K(X_{\mathrm{te}},Y)e^{-i\nu(X-X_{\mathrm{te}})} \tag{10}$$

Equation (7) therefore reads

$$4\pi\tilde{W}_p=\int\int_{\text{wing}} K\frac{\partial^2}{\partial Z^2}\left(\frac{e^{-i\kappa\xi}}{\xi}\right)\mathrm{d}S + \int\int_{\text{wake}} K_{\mathrm{te}}e^{-i\nu(X-X_{\mathrm{te}})}\frac{\partial^2}{\partial Z^2}\left(\frac{e^{-i\kappa\xi}}{\xi}\right)\mathrm{d}S \tag{11}$$

Lifting Surface Method

In the numerical technique developed in Ref. 17 for calculating the airloads on oscillating wings in rectilinear flight, the wing is divided into a number of panels and K is assumed to be constant over each panel. The wake is divided into a number of chordwise strips, and K over each strip is related to K_{te} as given in Eq. (10). Assume now that there are M panels along the chord of the wing and N panels along the span. For a panel mn the local doublet intensity K_{mn} is constant over the panel and may therefore be removed from the integration of Eq. (11) over that panel. Similarly, $K_{(\mathrm{te})n}$ may be expressed as K_{Mn} and removed from the integration of Eq. (11) over that strip. If the integrations in Eq. (11) are carried out over each panel and strip and then combined to form the entire surface integration, Eq. (11) may be written in influence coefficient form as

$$4\pi\tilde{W}_p=\sum_{m=1}^{M}\sum_{n=1}^{N}A_{p,mn}K_{mn}+\sum_{n=1}^{N}B_{p,n}K_{Mn} \tag{12}$$

where

$$A_{p,mn}=\int\int_{\text{panel } mn}\frac{\partial^2}{\partial Z^2}\left(\frac{e^{-i\kappa\xi}}{\xi}\right)\mathrm{d}S_{mn} \tag{12a}$$

and

$$B_{p,n}=\int\int_{\text{strip } n}e^{-i\nu(X-X_{\mathrm{te}})}\frac{\partial^2}{\partial Z^2}\left(\frac{e^{-i\kappa\xi}}{\xi}\right)\mathrm{d}S_n \tag{12b}$$

Here $A_{p,mn}$ represents the downwash velocity induced at P due to a unit intensity doublet at the panel mn, while $B_{p,n}$ represents the downwash velocity at P due to a unit intensity doublet in the wake strip n. For an $M\times N$ panel lifting surface, P takes $M\times N$ different values and the problem reduces to a set of simultaneous, linear algebraic equations

$$4\pi\{\tilde{W}\}=[C]\{K\} \tag{13}$$

where

$$C_{p,mn}=\begin{cases}A_{p,mn} & (m\neq M)\\ A_{p,mn}+B_{p,n} & (m=M)\end{cases}$$

The flow tangency condition, as detailed later, requires the downwash velocity induced by the doublets to equal the downward velocity of the wing at every point. Consequently, for prescribed wing motion and geometry, Eq. (13) may be solved for the doublet distribution K.

Application to Helicopter Rotors

The proper approach to the solution of Eq. (13) is to determine not only the doublet distribution but the wake geometry as well, since it is not known a priori. This additional requirement can increase the computational effort appreciably. However, for moderate to high aspect ratio fixed wings it has been found sufficiently accurate to specify the wake to be a planar vortex sheet, rather than to calculate its actual shape. A similar approach is therefore chosen for the rotor wake. That is, in the interest of reducing computer time but without compromising accuracy, the rotor wake geometry will be prescribed rather than calculated.

The difficulty, however, lies in choosing the proper wake shape for a given flight condition. The strip theory model is simple, but not physically realistic, since it ignores wake curvature. The classical wake model is an improvement, but it neglects tip vortex effects and the contraction of the wake beneath the rotor disk. Only Landgrebe's experimentally determined rotor wake model[15] includes all of these important effects. He models the wake as having a strong tip vortex and a weaker inboard vortex sheet and gives empirical equations for the radial and axial coordinates of both as functions of rotor geometry and operating conditions. Landgrebe gives the following equations for the axial ($\bar{Z}_T$) and radial ($\bar{r}$) coordinates of the tip vortex for a hovering rotor at any wake azimuth angle Ψ_w (see Figs. 1 and 2 for notation):

$$\bar{Z}_T=\begin{cases}k_1\Psi_w & (0\leq\Psi_w\leq 2\pi/\mathrm{NB})\\ (\bar{Z}_T)_{\Psi_w=2\pi/\mathrm{NB}}+k_2(\Psi_w-2\pi/\mathrm{NB}) & (\Psi_w\geq 2\pi/\mathrm{NB})\end{cases} \tag{14}$$

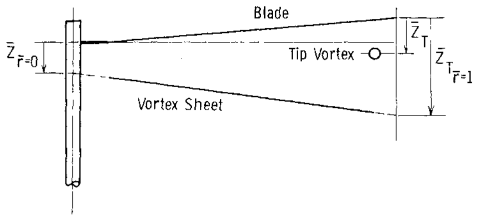

Fig. 1 View of wake cross section from trailing edge.

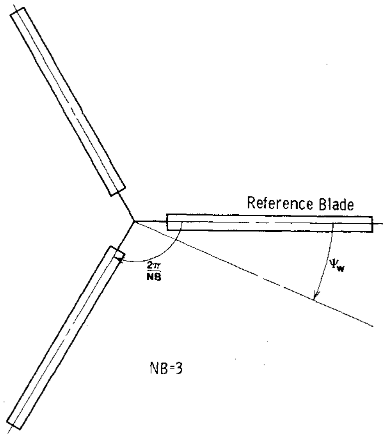

Fig. 2 View of rotor from above.

and

$$\bar{r}=0.78+0.22e^{-\lambda\Psi_w} \tag{15}$$

where

$$k_1=-0.25(C_T/\sigma+0.001\theta_1)$$

$$k_2=-(1.41+0.0141\theta_1)\sqrt{C_T/2}$$

$$\lambda=0.145+27C_T$$

Landgrebe assumes the cross section of the sheet to be linear and therefore gives equations for the intersection of the vortex sheet with the centerline of rotation ($\bar{Z}_{\bar{r}=0}$) and an imaginary surface described by the blade tip [$(\bar{Z}_T)_{\bar{r}=1}$]. The vortex sheet coordinates at any wake azimuth angle Ψ_w are given by the following equations:

$$\bar{Z}_{\bar{r}=0}=\begin{cases} 0 & (0\leq\Psi_w\leq\pi/2) \\ K_{2_{\bar{r}=0}}(\Psi_w-\pi/2) & (\Psi_w\geq\pi/2) \end{cases} \tag{16}$$

and

$$(\bar{Z}_T)_{\bar{r}=1}=\begin{cases} k_{1_{\bar{r}=1}}\Psi_w & (0\leq\Psi_w\leq 2\pi/\mathrm{NB}) \\ ((\bar{Z}_T)_{\bar{r}=1})_{\Psi_w=2\pi/\mathrm{NB}}+k_{2_{\bar{r}=1}}(\Psi_w-2\pi/\mathrm{NB}) & (\Psi_w\geq 2\pi/\mathrm{NB}) \end{cases} \tag{17}$$

where

$$k_{1_{\bar{r}=1}}=-2.2\sqrt{C_T/2}$$

$$k_{2_{\bar{r}=1}}=-2.7\sqrt{C_T/2}$$

$$k_{2_{\bar{r}=0}}=(\theta_1/128)(0.45\theta_1+18)\sqrt{C_T/2}$$

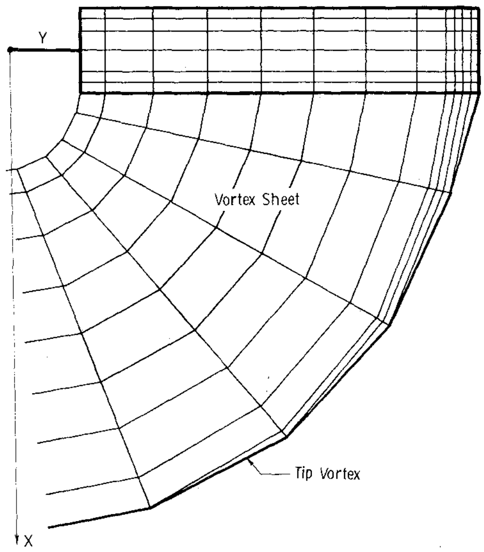

Fig. 3 Rotor and wake model.

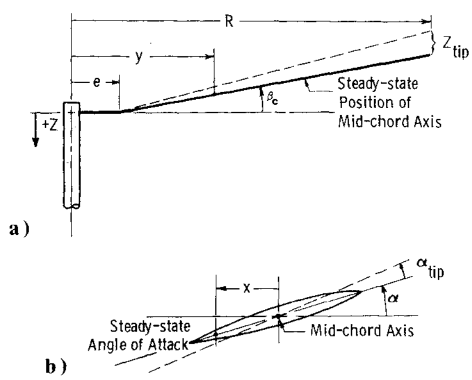

Fig. 4 Components of rotor blade motion: a) view from trailing edge; b) view from blade tip.

In this report these equations were used with only slight modifications; however, two refinements were made to the model for the present study. The first was to extend the outer vortex sheet boundary to the tip vortex, since there is likely a physical connection between the two. The second was to simulate the roll up of the vortex sheet into a tip vortex by gradually combining the outer vortex sheet wake strips into a single strip with the combined strength of the composite strips. This process was done over an arbitrarily chosen one-sixth rotor revolution to insure that the tip vortex reached full strength before passing beneath the following blade. The portion of the wake which combined to form the tip vortex was determined by the spanwise location of the peak load on the rotor blade, and since the peak load is generally near the 85-90% radius position, all wake strips outboard of that location were blended into the tip vortex. Furthermore, the outermost segment of the strips in this region was assigned tip vortex coordinates, while all others were given vortex sheet coordinates. It was also assumed that the vortex sheet contracted radially at the same rate as the tip vortex.

As suggested by Jones and Moore,[17] the blade surface is divided into a number of small panels and the panel size is smaller in regions where K varies most rapidly, i.e., near the blade edges. The freestream velocity is assumed to be constant across a panel and equal to the velocity at the geometric centroid of the panel. This velocity varies with span due to the nature of the rotor flowfield. Extending from each trailing-edge panel is a wake strip whose coordinates are determined by Landgrebe's equations (Fig. 3 shows the panel approximation of the rotor blade and the modified wake model).

Calculation of Influence Coefficients

Equation (13) can be solved for K at a discrete number of points on the surface which, in the present study, are arbitarily placed at the geometric centroid of each panel. The influence of a surface panel on a collocation point is given by Eq. (12a), which is evaluated numerically using a two-dimensional Gaussian quadrature. The influence of a wake strip on a collocation point is given by Eq. (12b) with the following modification: implicit in the use of Eq. (10) for enforcing the zero-pressure condition in the wake is the assumption that the local streamlines are in the direction of the positive X axis. In a linearized sense this is true for fixed wings. However, for rotary wings the streamlines are directed along roughly helical paths beneath the rotor disk. To reflect this difference Eq. (10) is therefore modified to

$$K(S)=K(S_{\mathrm{te}})e^{-i\nu(S-S_{\mathrm{te}})} \tag{18}$$

where S is the distance measured along the centerline of any wake strip. Of course, Eq. (12b) must be changed in accordance with Eq. (18). The effect that a particular wake strip has on a collocation point is therefore computed by adding the effect that each panel in the strip has on that point using the modified form of Eq. (12b). As with the surface panels, the integrations are carried out with a two-dimensional Gaussian quadrature.

Surface Boundary Condition

The vertical displacement of the blade is assumed to have a steady-state component due to coning and angle of attack, and an unsteady component due to flapping and twisting about this steady position, i.e.,

$$\zeta=\zeta_s+\zeta_f' e^{i\omega T}+\zeta_t' e^{i\omega T} \tag{19}$$

It can be seen from Fig. 4 that

$$\zeta_s=(e-y)\beta_c+x\alpha \tag{20a}$$

$$\zeta_f'=f(y)z_{\mathrm{tip}} \tag{20b}$$

$$\zeta_t'=F(y)\alpha_{\mathrm{tip}} \tag{20c}$$

The relations between the downwash velocity $\tilde{w}_p$ and ζ, and $\tilde{w}_p$ and the transformed downwash velocity $\tilde{W}_p$ are, respectively,

$$\tilde{w}_p=\frac{\partial\zeta}{\partial t}+U\frac{\partial\zeta}{\partial x} \tag{21}$$

and

$$\tilde{W}_p=\tilde{w}_p\frac{e^{-i(\lambda X+\omega T)}p}{U_t\beta_p} \tag{22}$$

Equations (19) through (22) are combined to give

$$\tilde{W}_p=\tilde{W}_{sp}+\tilde{W}_{zp}+\tilde{W}_{\alpha p} \tag{23}$$

where

$$\tilde{W}_{sp}=(y_p/R\beta_p)\alpha_p \tag{23a}$$

$$\tilde{W}_{zp}=\frac{f(y)z_{\mathrm{tip}}e^{-i\lambda_p X_p}}{R\beta_p}(i\epsilon) \tag{23b}$$

$$\tilde{W}_{\alpha p}=\frac{F(y)\alpha_{\mathrm{tip}}e^{-i\lambda_p X_p}}{R\beta_p}(y_p+i\epsilon x_p) \tag{23c}$$

The solution for steady flow is obtained by setting $\nu=0$ and $\kappa=0$ in Eqs. (12a) and (12b) and using Eqs. (13) and (23a). Similarly, the solutions for flapping and twisting are obtained by using Eq. (23b) and Eq. (23c), respectively, in Eq. (13).

Aerodynamic Loads

Equation (9), the linearized expression for the lift in transformed coordinates, is modified to

$$\tilde{l}(X,Y,T)=\rho UU_t\left(i\nu K+\frac{\partial K}{\partial X}\right)e^{i(\lambda X+\omega T)} \tag{24}$$

By integrating Eq. (24) along the chord, the local lift and moment per unit span may be expressed as

$$L'=\rho U^2 l\left(\frac{R}{y}\right)\left[\bar{K}_{\mathrm{te}}-i\omega\int_{-l}^{+l}\bar{K}\mathrm{d}X\right]e^{i\omega T} \tag{25}$$

$$M_{c/2}'=-\rho U^2 l^2\left(\frac{R}{y}\right)\left[\bar{K}_{\mathrm{te}}-\int_{-l}^{+l}\bar{K}\mathrm{d}X+i\omega\int_{-l}^{+l}\bar{K}X\mathrm{d}X\right]e^{i\omega T} \tag{26}$$

where $\bar{K}=Ke^{i\lambda X}$. The unsteady lift and moment coefficients for flapping and twisting are expressed as

$$C_L=\frac{L'}{\rho U^2 l}=C_{Lz}z_{\mathrm{tip}}'+C_{L\alpha}\alpha_{\mathrm{tip}} \tag{27}$$

$$C_{mc/2}=\frac{M_{c/2}'}{\rho U^2 l^2}=C_{Mz}z_{\mathrm{tip}}'+C_{M\alpha}\alpha_{\mathrm{tip}} \tag{28}$$

where $z_{\mathrm{tip}}'=z_{\mathrm{tip}}/l$. It should be noted that C_{Lz}, $C_{L\alpha}$, C_{Mz}, and $C_{M\alpha}$ are complex quantities.

Solution Procedure

For a given rotor geometry and flight condition, blade element theory is used to calculate an initial guess to the rotor thrust coefficient C_T. Based on this value of C_T and the initial conditions, an initial wake shape is prescribed using the modified Landgrebe model. The resultant steady-state airloads are then calculated and an improved guess for C_T is made. If this second value differs appreciably from the first, a new wake geometry is prescribed based on the new value of C_T and a new set of steady-state airloads is calculated. This process is repeated until a wake geometry exists which is compatible with the steady-state load distribution, i.e., $\Delta C_T\to 0$. The unsteady aerodynamic derivatives are then calculated based on this converged wake geometry.

Results

Steady airloads and unsteady aerodynamic derivatives were calculated for an XH-51A helicopter rotor in hover. This rotor was chosen because experimental data [19] for the steady-state load distribution was available for comparison with theory. The blade geometry and flight conditions were

$$\mathrm{NB}=4,\quad R=17.5\ \mathrm{ft}$$

$$c=1.08\ \mathrm{ft},\quad y_{\mathrm{co}}=2.33\ \mathrm{ft}$$

$$\theta_l=-5\ \mathrm{deg},\quad \theta_r=10.61\ \mathrm{deg}$$

$$N_R=355\,(M_{\mathrm{tip}}=0.58)$$

In the unsteady case the blades were assumed to undergo rigid flapping and torsional motion such that

$$f(y)=\begin{cases}0 & (y\le e)\\ (y-e)/(R-e) & (y\ge e)\end{cases}$$

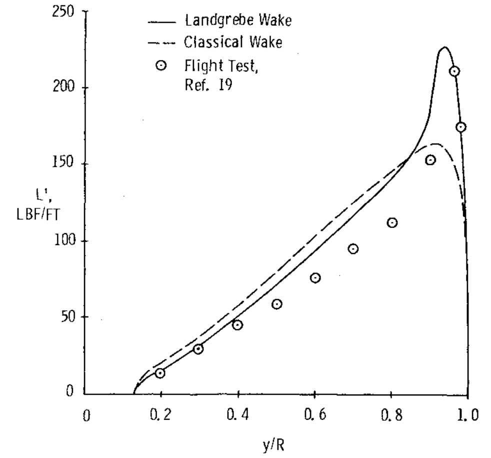

Fig. 5 Lift per unit span, XH-51A helicopter rotor.

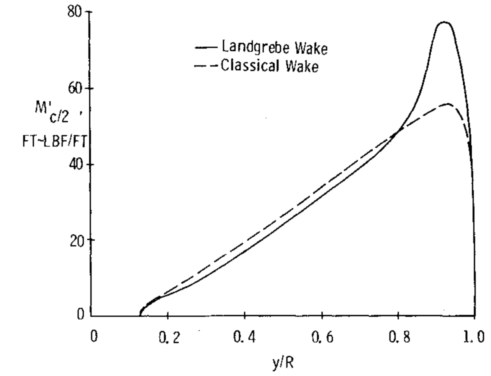

Fig. 6 Moment per unit span, XH-51A helicopter rotor.

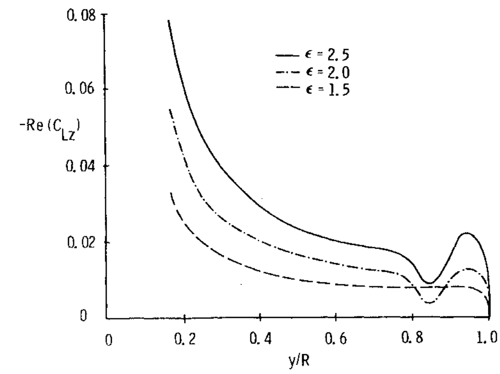

Fig. 7 Real part of lift due to flapping.

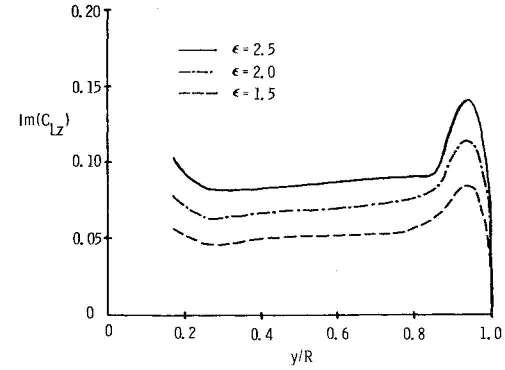

Fig. 8 Imaginary part of lift due to flapping.

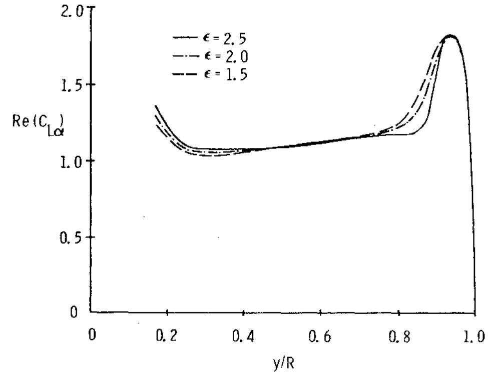

Fig. 9 Real part of lift due to torsion.

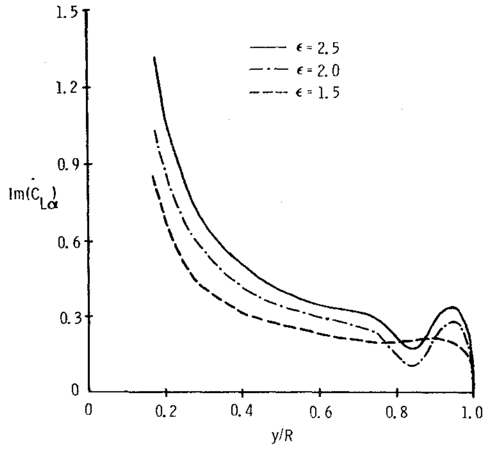

Fig. 10 Imaginary part of lift due to torsion.

and $F(y) = 1$. Figures 5 and 6 show the calculated lift and moment distributions for the XH-51A using the present theory with the classical and Landgrebe wake models. Both models overpredict the overall blade lift, although Landgrebe's model predicts the loading trends more accurately, specifically the load spike near the tip due to the tip vortex. The mean value for C_T for the classical model was 0.00577 and that for the Landgrebe model was 0.00584, while the experimental value was roughly 0.005 – a difference of 15 to 17% between theory and experiment. This difference may be due to the approximate nature of the present method, i.e., discretizing the linear spanwise velocity field into constant velocity segments. No comparison was made between the theoretical and experimental moment distributions since the measured data were referenced to an unspecified axis. It might be expected, however, that Landgrebe's model would give better results in the tip region than would the classical model. The number of wake revolutions used in this study was varied from one to four with no appreciable change in the overall thrust or character of the leading curves, but with a drastic increase in computational time. The displayed results are therefore those obtained using a single wake revolution. For lightly loaded rotors (where the rotor wake is closer to the blade), it may be necessary to include more wake revolutions to get accurate results. The calculation of the steady-state loads using either wake model required approximately 36 seconds of CPU time in G-level FORTRAN on an Amdahl 470V/6 computer.

Based on the steady-state results, only the Landgrebe model was used in calculating the unsteady aerodynamic derivatives. The results for three frequency ratios are shown in Figs. 7-14. Evident in each of these figures is the strong tip vortex influence on the loading over the outer 20% of the blade. In the present study no attempt is made to explain the variation of these quantities as a function of frequency ratio or its significance in flutter analysis. However, based on the

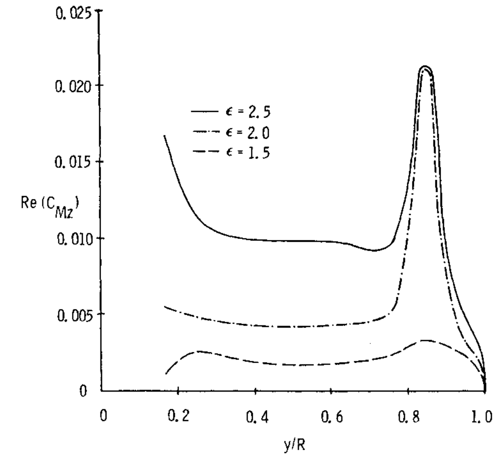

Fig. 11 Real part of moment due to flapping.

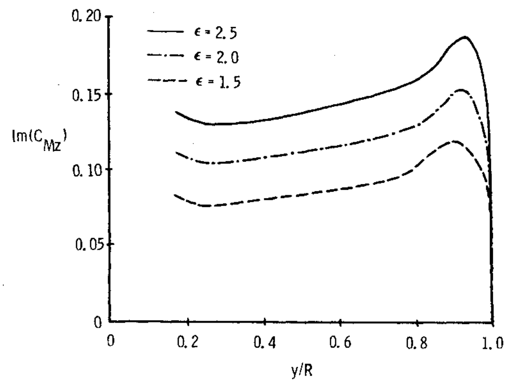

Fig. 12 Imaginary part of moment due to flapping.

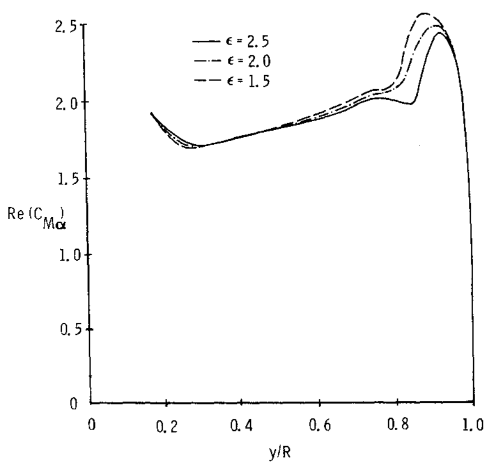

Fig. 13 Real part of moment due to torsion.

reasonable correlation between steady-state theoretical and experimental loading using the Landgrebe model, it is hoped that the computed unsteady aerodynamic derivatives will also be reasonably accurate. In the future these results will be compared with those of strip theory and classical wake model representations and applied to investigate their effect on aeroelastic stability boundaries as was done in Ref. 8. The calculation of the steady-state airloads and wake geometry and the resulting unsteady aerodynamic derivatives required approximately 2.8 minutes of CPU time in G-Level FORTRAN on an Amdahl 470V/6 computer.

Conclusions

A velocity potential lifting surface method has been used in conjunction with a realistic rotor wake model to compute the

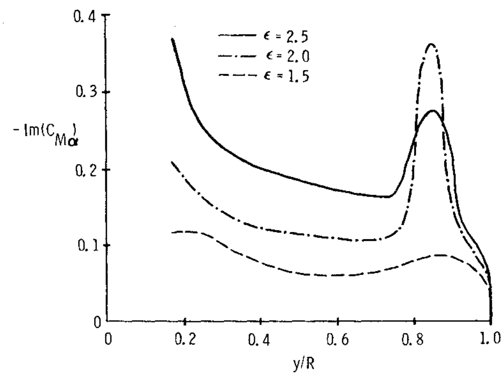

Fig. 14 Imaginary part of moment due to torsion.

steady airloads and unsteady aerodynamic derivatives for an arbitrary hovering rotor in compressible flow. The theoretical results for the spanwise lift distribution compare reasonably well with experimental data for four-bladed rotors, suggesting that unsteady loads calculated with the same wake geometry may also be reasonably accurate. With the proper choice of flapping and torsional modes, the present method could be used to generate unsteady aerodynamic derivatives for use in flutter analysis.

Acknowledgment

This work was supported by the U.S. Army Research Office under Grants DAHC04-74-G0184 and DAAG29-76-G-0241. The authors gratefully acknowledge Robert E. Singleton, Chief, Fluid Mechanics Branch, Army Research Office, for his support of this research.

References

[1]Jones, W. P., McCrosky, W. J., and Costes, J. J., "Unsteady Aerodynamics of Helicopter Rotor Blades," NATO AGARD Rept. No. 595, April 1972.

[2]Loewy, R. G., "A Two-Dimensional Approximation to the Unsteady Aerodynamics of Rotary Wings," *Journal of the Aeronautical Sciences*, Vol. 24, Feb. 1957, pp. 81-92.

[3]Jones, J. P., "The Influence of the Wake on the Flutter and Vibration of Rotor Blades," *Aeronautical Quarterly*, Vol. IX, Aug. 1958, pp. 258-286.

[4]Timman, R. and Van de Vooren, A. I., "Flutter of a Helicopter Rotor Rotating in Its Own Wake," *Journal of the Aeronautical Sciences*, Vol. 24, Sept. 1957, pp. 694-702.

[5]Jones, W. P. and Rao, B. M., "Compressibility Effects on Oscillating Rotor Blades in Hovering Flight," *AIAA Journal*, Vol. 8, Feb. 1970, pp. 321-329.

[6]Jones, W. P., "The Oscillating Airfoil in Subsonic Flow," British Aeronautical Research Council, R&M No. 2921, 1956.

[7]Hammond, C. E., "Compressibility Effects in Helicopter Rotor Blade Flutter," Georgia Institute of Technology, School of Aerospace Engineering, GITAER Rept. 69-4, Dec. 1969.

[8]Friedmann, P. and Yuan, C., "Effect of Modified Aerodynamic Strip Theories on Rotor Blade Aeroelastic Stability," *Proceedings of the AIAA/ASME/SAE 17th Structures, Structural Dynamics and Materials Conference*, May 1976, pp. 398-411.

[9]Jones, W. P. and Rao, B. M., "Tip Vortex Effects on Oscillating Rotor Blades in Hovering Flight," *AIAA Journal*, Vol. 9, Jan. 1971, pp. 106-113.

[10]Miller, R. H., "Rotor Blade Harmonic Air Loading," *AIAA Journal*, Vol. 2, July 1964, pp. 1254-1469.

[11]Piziali, R. A., "A Method for Predicting the Aerodynamic Loads and Dynamic Response of Rotor Blades," USAAV-LABS Tech. Rept. 65-74, Jan. 1966, AD 628583.

[12]Sadler, S. G., "A Method for Predicting Helicopter Wake Geometry, Wake Induced Flow and Wake Effects on Blade Airloads," presented at the 27th Annual National V/STOL Forum of the American Helicopter Society, Washington, D. C., May 1972.

[13]Rao, B. M. and Jones, W. P., "Application to Rotary Wings on a Simplified Aerodynamic Lifting Surface Theory for Unsteady Compressible Flow," *Proceedings of the AHS/NASA-AMES Specialist's Meeting on Rotorcraft Dynamics*, Feb. 1974.

[14]Jenney, D. S., Olson, J. R. and Landgrebe, A. J., "A Reassessment of Rotor Hovering Performance and Wake Geometry Characteristics," USAAMRDL Tech. Rept. 71-24, June 1971.

[15]Landgrebe, A. J., "An Analytical and Experimental Investigation of Helicopter Rotor Hover Performance and Wake Geometry Characteristics," USAAMRDL Tech. Rept. 71-24, June 1971.

[16]Schatzle, P. R., "Unsteady Airloads on Rotary Wings in Subsonic, Compressible Flow," Master's Thesis, Texas A&M University, May 1976.

[17]Jones, W. P. and Moore, J. A., "Simplified Aerodynamic Theory of Oscillating Thin Surfaces in Subsonic Flow," *AIAA Journal*, Vol. 11, Sept. 1973, pp. 1035-1039.

[18]Jones, W. P., "Oscillating Wings in Compressible Subsonic Flow," British Aeronautical Research Council, R&M No. 2855, Oct. 1951.

[19]Bartsch, E. A., "In-Flight Measurements and Correlation with Theory of Blade Airloads and Responses on the XH-51A Compound Helicopter Rotor – Volume 1: Measurement and Data Reduction of Airloads and Structural Loads," USAAVLABS TR-68-22A, May 1968.